Aperiodic-Tiling-Based Mushroom-Type High-Impedance Surfaces

Ilaria Gallina, Alessandro Della Villa, Vincenzo Galdi, *Senior Member, IEEE*, Vincenzo Pierro, Filippo Capolino, *Senior Member, IEEE*, Stefan Enoch, Gérard Tayeb, and Giampiero Gerini, *Member, IEEE*

***Abstract*—This letter deals with a study of *aperiodically ordered* textured (mushroom-type) high-impedance surfaces (HISs), and their possible application as artificial-magnetic-conductor ground-planes for low-profile directive antennas. In this framework, results from full-wave simulations are presented in order to characterize the electromagnetic response (in terms of impedance matching, directivity, and surface-wave suppression) of selected configurations based on representative categories of aperiodic tilings, and compare them with those of standard periodic HISs.**

***Index Terms*—Antenna ground-planes, artificial impedance surfaces, artificial magnetic conductors (AMCs), quasi-crystals.**

I. Introduction and Background

DURING the last decade, artificial high-impedance surfaces (HISs) have been extensively investigated and proposed as effective ground planes for improving the electrical and radiative responses of low-profile planar antennas (see [1] for a collection of recent results and applications). The main interest originates from their potential capabilities, within certain frequency ranges, of reflecting electromagnetic (EM) waves with no phase reversal, i.e., behaving as an *artificial magnetic conductor* (AMC), and suppressing the surface-wave (SW) propagation [2].

Nearly all available examples of HIS configurations are based on particular textures, such as corrugations, mushroom-type protrusions, etc., arranged *periodically*, for which the EM response is well understood (see, e.g., [3] and [4]). However, inspired by the discovery in solid-state physics of "quasi- crystals" [5], [6] and by the theory of "aperiodic tilings" [7], it has been shown in other artificial-material contexts (e.g., photonic crystals, arrays of subwavelength holes, etc.) that spatial periodicity is *not essential* to achieve anomalous EM effects like bandgaps, negative refraction and superlensing, directive emission, enhanced transmission, etc. (see [8]–[17] and the references therein for a sparse sampling). In fact, judicious exploitation of the additional degrees of freedom and higher (local, statistical) rotational symmetries potentially available in *aperiodically ordered* geometries can be exploited to achieve larger bandgaps, lower and/or multiple frequencies of operation, higher isotropy, richer and more frequency-selective defect states, etc. In this framework, a novel mushroom-type HIS configuration was recently proposed in [18], based on a *quasi-periodic* octagonal (Ammann-Beenker) tiling geometry [7]. Experimental and numerical studies of this structure revealed a very interesting EM response, in terms of multiple frequencies of operation, highly directive radiation from a small electric dipole laid on it, and broadband suppression of the transverse-electric SW.

In this letter, in order to gain further insight into the underlying phenomenology and potentials, we address a comparative study of various HIS configurations with aperiodically ordered mushroom-type textures, based on representative categories of aperiodic tilings. Our study is principally aimed at exploring to what extent the intriguing results observed in [18] are restricted to that particular (octagonal) geometry, or instead they are representative of intrinsic properties of rather generic aperiodically ordered configurations. In this framework, we study three aperiodic representative finite-size HIS ground-planes, as well as the well-known periodic (square) counterpart. Via full-wave simulations, we compare their responses in terms of the radiation (return loss and directivity) from a small electric dipole laid on them, and SW attenuation.

II. Geometry and Parameters

The three representative aperiodic tilings considered are as follows.

- *Octagonal* (Ammann-Beenker), as in [18], with square- and rhombus-shaped tiles, and eightfold symmetry [7].
- *Dodecagonal*, with square- and equilater-triangle-shaped tiles, and 12-fold symmetry [19].
- *Penrose*, with thick/thin-rhombus-shaped tiles, and fivefold symmetry [7].

The octagonal and Penrose tilings are generated via "cut-and-projection" algorithms [7], whereas the dodecagonal tiling is generated using the Stampfli iterative construction [19]. As a reference configuration, we also consider a standard periodic (square) geometry, whose EM response is well known [2]–[4]. Note that standard concepts and tools typically utilized for the study of periodic HIS configurations ("unit cell," band-structure, Brillouin zone, etc.) *cannot* be applied to the aperiodic scenarios of interest here. Therefore, our study involves *finite-size* HIS structures, obtained by cutting suitably sized regions

Manuscript received July 20, 2007; revised December 22, 2007. This work was supported in part by the Italian Ministry of Education and Scientific Research (MIUR) under the PRIN-2006 Grant on "Study and realization of metamaterials for electronics and TLC applications," and by the EU project METAMORPHOSE (FP6/NMP3-CT-2004-500252) Network of Excellence.

I. Gallina, V. Galdi, and V. Pierro are with the Waves Group, Department of Engineering, University of Sannio, I-82100 Benevento, Italy (e-mail: ilaria.gallina@unisannio.it; vgaldi@unisannio.it; pierro@unisannio.it).

A. Della Villa and F. Capolino are with the Department of Information Engineering, University of Siena, I-53100 Siena, Italy (e-mail: dellavilla@gmail.com; capolino@dii.unisi.it).

S. Enoch and G. Tayeb are with the Institut Fresnel, CNRS, Aix-Marseille Université, Faculté des Sciences et Techniques, case 161, 13397 Marseille cedex 20, France (e-mail: stefan.enoch@fresnel.fr, gerard.tayeb@fresnel.fr).

G. Gerini is with the TNO Defence, Security and Safety, 2509 JG The Hague, The Netherlands, and also with the Department of Electrical Engineering, Technical University of Eindhoven, 5612 AZ Eindhoven, The Netherlands (e-mail: giampiero.gerini@tno.nl).

Digital Object Identifier 10.1109/LAWP.2008.916674

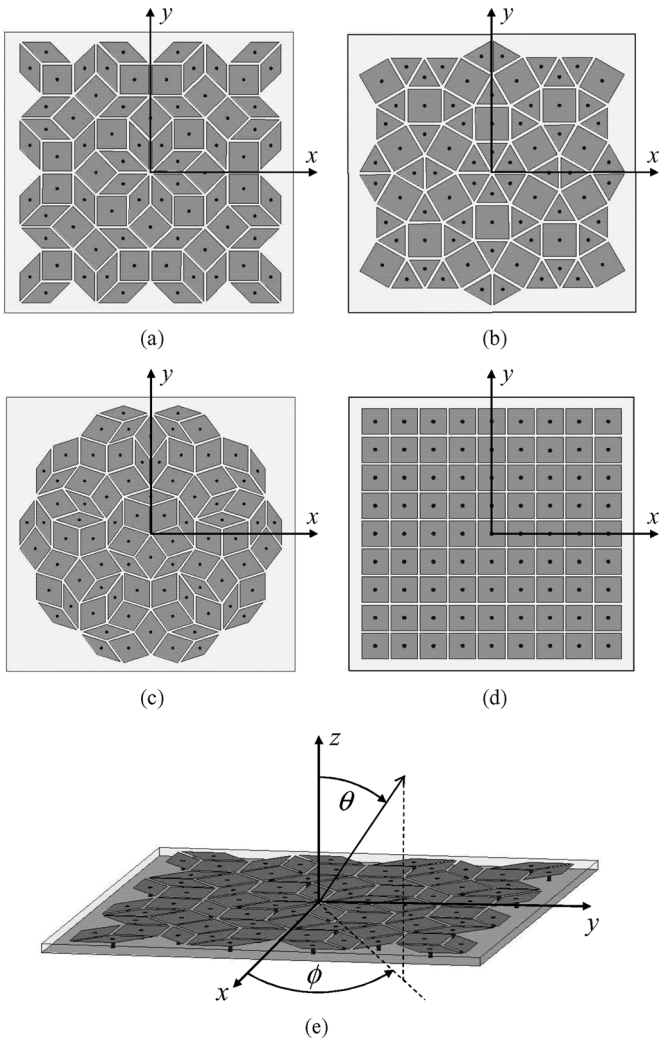

Fig. 1. HIS geometry and parameters. (a)—(d) Top view. (e) Three-dimensional view (octagonal). Metallic (copper) patches of sidelength $a_{\rm patch}$ are laid with a 0.7-mm gap on a metal-backed dielectric substrate of thickness 1.6 mm and relative permittivity $\epsilon_r = 2.2$, and are connected to the ground plane by metallic vias with diameter 0.7 mm. Also shown are the Cartesian and spherical reference coordinate systems, with origin at the local symmetry center. (a) Octagonal ($a_{\rm square} = 7.6$ mm, $a_{\rm rhombus} = 7.3$ mm, total size: 70×70 mm^2). (b) Dodecagonal ($a_{\rm square} = 7.6$ mm, $a_{\rm triangle} = 7.1$ mm, total size: 62×62 mm^2). (c) Penrose ($a_{\rm thick} = 7.6$ mm, $a_{\rm thin} = 7.2$ mm, total size: 76×76 mm^2). (d) Periodic ($a_{\rm square} = 7.6$ mm, total size: 76×76 mm^2).

of the above tilings (preserving the local symmetry centers), and placing metallic (copper) patches shaped according to the tiles on top of a 1.6-mm-thick dielectric substrate with relative permittivity $\epsilon_r = 2.2$ (RT/duroid 5880) backed by a metallic ground plane. The patches are suitably scaled, so as to guarantee a constant 0.7-mm gap between them, and are connected to the ground plane by metallic vias of diameter 0.7 mm. The patch characteristic sizes are chosen as in [18], so as to facilitate direct comparison with our results (at least for the octagonal geometry), whereas the total structure sizes are set by our current computational resource limitations. For the various geometries, these values were tuned so as to maintain the same spacing between the metal patches and a comparable number of patches.

Fig. 1(a)–(d) shows the top view of the four HIS configurations under analysis. For the octagonal case, a three-dimensional view is also displayed in Fig. 1(e).

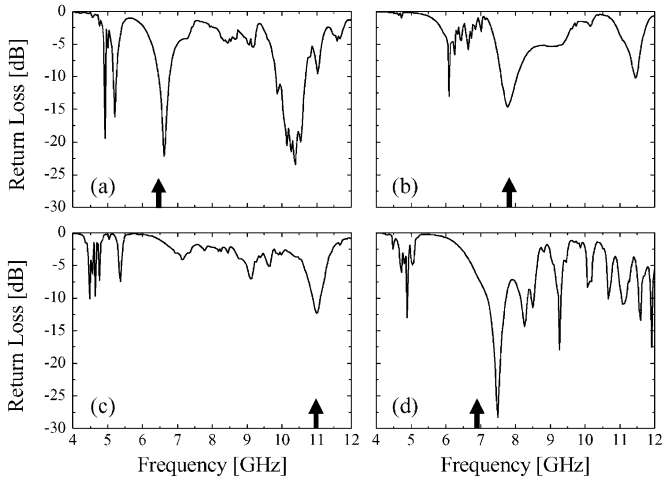

Fig. 2. Geometry and parameters as in Fig. 1. Return loss ($|S_{11}|$) of an x-directed 16-mm-long electric dipole placed at $x = y = 0, z = 0.7$ mm (i.e., right above the local symmetry center). (a) Octagonal. (b) Dodecagonal. (c) Penrose. (d) Periodic. Arrows mark the frequency values where a reasonable tradeoff between RL and broadside directivity (see Fig. 3) was observed.

III. Representative Results

For finite-size HIS structures, the AMC behavior can be meaningfully ascertained by studying the radiation characteristics of a small electric dipole, laid parallel to the surface at a very close distance. Recalling basic image theory, the dipole will radiate very poorly when the surface is acting as standard (electric) ground plane, and much more efficiently when the surface is acting as an AMC, resulting in a low return-loss (RL) [2].

In our simulations, we placed a 16-mm-long electric dipole, parallel (x-directed) and very close to the surface ($x = y = 0, z = 0.7$ mm, i.e., right above its local symmetry center), and computed via a full-wave commercial software package [20] the RL ($|S_{11}|$) spectra for the various configurations. Results are shown in Fig. 2 within the frequency range 4–12 GHz. For each geometry, one observes some (more or less pronounced) dips in the RL spectrum, corresponding to AMC-type behavior. In particular, the results for the octagonal HIS [Fig. 2(a)] agree fairly well with those observed in [18], with three main dips at frequencies ~ 5, 6.5, and 10 GHz. Qualitatively similar behaviors, with less pronounced and frequency-shifted dips, are observed for the dodecagonal [Fig. 2(b)] and the Penrose [Fig. 2(c)] geometries, whereas the periodic HIS [Fig. 2(d)] turns out to exhibit more pronounced, but narrower, dips.

We then studied the radiation characteristics within the AMC bands. For conventional (metallic) ground planes, SWs can propagate along the metal-air interface and eventually radiate when reaching discontinuities (e.g., corners, edges), resulting in the appearance in the radiation pattern of ripples in the forward direction, and a degradation of the front-to-back ratio. It has been shown that periodically textured HIS ground-planes capable of strongly attenuating SW propagation can overcome these problems, thereby significantly improving the radiation pattern quality [2]. Fig. 3(a)–(d) shows some representative radiation patterns observed for the 16-mm-long electric dipole laid on the four HIS ground planes, at frequencies (marked as

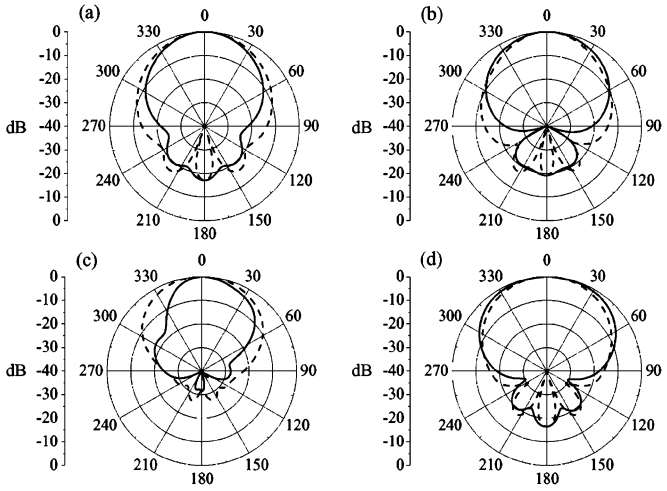

Fig. 3. As in Fig. 2, but radiation patterns at selected frequency values (marked by arrows in Fig. 2). (a) Octagonal (6.49 GHz, $\mathrm{RL} = -11.2$ dB). (b) Dodecagonal (7.82 GHz, $\mathrm{RL} = -14.2$ dB). (c) Penrose (11 GHz, $\mathrm{RL} = -12.3$ dB). (d) Periodic (6.89 GHz, $\mathrm{RL} = -6.6$ dB). Solid curves: $\phi = 0°$ plane; dashed: $\phi = 90°$ plane.

arrows in Fig. 2) chosen so as to provide a reasonable tradeoff between high broadside directivity and low RL. As expected, one observes the lack of ripples in the forward direction and the low backward radiation ($\lesssim -15$ dB). Again, our results qualitatively confirm the rather high broadside directivity observed in [18] for the octagonal HIS [Fig. 3(a)], with half-power beamwidths of 52° and 64° in the principal planes $\phi = 0°$ and $\phi = 90°$, respectively. The lower directivity, as compared to that in [18], can be attributed to the smaller structure size considered here. Qualitatively similar results are observed for the dodecagonal [Fig. 3(b)] and Penrose [Fig. 3(c)] geometries. For the Penrose HIS, the chosen frequency (11 GHz) is considerably higher than for the other geometries; around lower-frequency dips, either the broadside directivity or the RL were found to be unsatisfactory. Moreover, the slight pattern asymmetry is attributable to the breaking of the underlying fivefold symmetry due to the presence of the dipole. For the periodic HIS in the considered parametric configuration [Fig. 3(d)], a moderately lower directivity was observed, with beamwidths of 90° ($\phi = 0°$ plane) and 70° ($\phi = 90°$ plane). Also, the RL is considerably higher than the aperiodic cases; at frequencies closer to the main RL dip [cf. Fig. 2(d)] the radiation patterns were found to exhibit a main-lobe splitting, with poorer broadside radiation (see, e.g., Fig. 4).

Finally, as in [18], we studied more in detail the SW propagation, for both transverse electric (TE) and magnetic (TM) polarizations. For the TE case, we placed two y-directed 16-mm-long electric dipoles laid 0.25 mm above the HIS, at two opposite ends, and computed the transmission ($|S_{12}|$) spectra. For the TM case, we considered two z-directed 8-mm-long monopoles. Results are shown in Fig. 5(a) and (b), respectively (with the simulation schematics illustrated in the insets), for the four geometries under study. In the TE case [Fig. 5(a)], the aperiodic HIS configurations exhibit several bandgaps characterized by strong SW attenuation, as observed in [18] for the octagonal geometry. Conversely, the periodic HIS exhibits only one bandgap

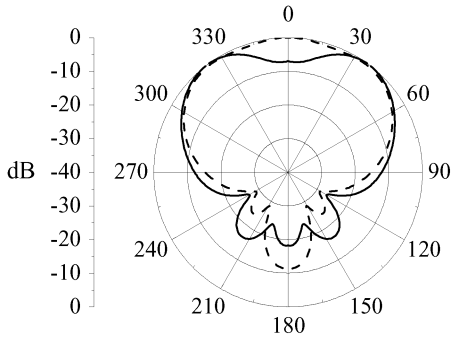

Fig. 4. As in Fig. 3(d), but at 7.5 GHz ($\mathrm{RL} = -28$ dB).

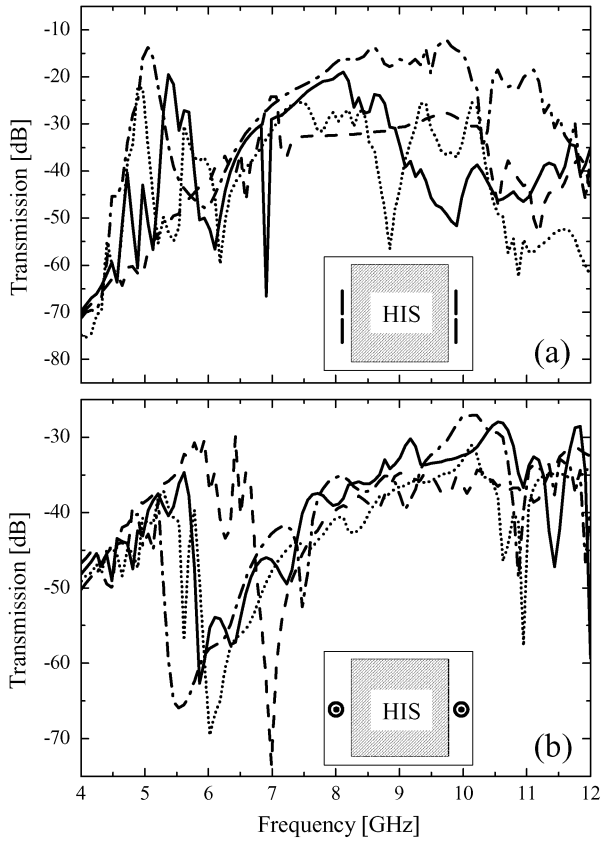

Fig. 5. SW transmission ($|S_{12}|$) spectra for the HIS configurations in Fig. 1 for (a) TE and (b) TM polarizations (simulation schematics are illustrated in the insets). Solid curves: octagonal (probe separation: 72 mm); dashed: dodecagonal (probe separation: 64 mm); dotted: Penrose (probe separation: 78 mm); dash-dotted: periodic (probe separation: 78 mm).

with significant SW attenuation. In the TM case [Fig. 5(b)], one observes the presence of several dips and similar attenuation levels for all the geometries. These results were found to be rather robust with respect to variations in the probe positions.

IV. Conclusions and Open Issues

In this letter, we have presented a comparative study of the EM properties of finite-size HIS ground-planes based on aperiodically ordered mushroom-type textures. We have considered three representative aperiodic-tiling geometries (octagonal, dodecagonal, and Penrose) and a standard periodic (square) geometry, and compared their performance as ground-planes for low-profile directive antennas, in terms of return-loss, radiation

properties, and SW suppression. Our results, based on full-wave simulations, confirm those already observed in [18] (in connection with the octagonal geometry) and reveal the inherent suitability of more general aperiodic-tiling-based geometries to HIS applications. The availability of further and still largely unexplored degrees of freedom in the lattice geometry could open up new perspectives in the HIS design. Indeed, aperiodically ordered HIS structures seem potentially capable of yielding multiple AMC bands, strong attenuation of TE and TM SW propagation, and directive broadside radiation.

It should be emphasized that no effort was made at this stage to optimize the various parametric configurations, and to assess the actual superiority of aperiodically ordered HISs as compared to standard periodic configurations. In this connection, more comprehensive parametric studies and deeper understanding of the underlying phenomenologies are needed for a fruitful exploitation of the aforementioned geometry-related degrees of freedom in the engineering of bandgap and AMC properties. Among the open issues, currently under investigation, it is worth mentioning the following.

- The role of local order and symmetry. In this connection we are planning a comprehensive parametric study involving various randomly cut tiling realizations (not necessarily preserving the local symmetry center) of different sizes, and with different source positions and orientations. Also of interest, is the study of periodic Archimedean-type tiling geometries [21] featuring different (e.g., square- and equilater-triangle-shaped) tiles, so as to separate the aperiodicity effects from the presence of different tile shapes (see also the discussion in [18]).
- The study of possible mechanisms for performance control and optimization.
- The study of aperiodically ordered uniplanar HIS configurations.

ACKNOWLEDGMENT

The authors wish to thank Prof. C. T. Chan and Z. Hang of the Hong Kong University of Science and Technology for useful suggestions.

REFERENCES

[1] P.-S. Kildal, A. Kishk, and S. Maci, Eds., *IEEE Trans. Antennas Propag.*, vol. 53, Special Issue on Artificial Magnetic Conductors, Soft/Hard Surfaces, and other Complex Surfaces, no. 1, Jan. 2005.

[2] D. Sievenpiper, L. Zhang, R. F. J. Bross, N. G. Alexópolous, and E. Yablonovitch, "High-impedance electromagnetic surfaces with a forbidden frequency band," *IEEE Trans. Microw. Theory Tech.*, vol. 47, no. 11, pp. 2059–2074, Nov. 1999.

[3] F. Yang and Y. Rahmat-Samii, "Reflection phase characterizations of the EBG ground plane for low profile wire antenna applications," *IEEE Trans. Antennas Propag.*, vol. 51, no. 10, pt. I, pp. 2691–2703, Oct. 2003.

[4] H. Mosallaei and K. Sarabandi, "Antenna miniaturization and bandwidth enhancement using a reactive impedance substrate," *IEEE Trans. Antennas Propag.*, vol. 52, no. 9, pp. 2403–2414, Sep. 2004.

[5] D. Shechtman, I. Blech, D. Gratias, and J. W. Cahn, "Metallic phase with long-range orientational order and no translation symmetry," *Phys. Rev. Lett.*, vol. 53, no. 20, pp. 1951–1953, Nov. 1984.

[6] D. Levine and P. J. Steinhardt, "Quasicrystals: A new class of ordered structures," *Phys. Rev. Lett.*, vol. 53, no. 26, pp. 2477–2480, Dec. 1984.

[7] M. Senechal, *Quasi-Crystals and Geometry*. Cambridge, U.K.: Cambridge Univ. Press, 1995.

[8] Y. S. Chan, C. T. Chan, and Z. Y. Liu, "Photonic band gaps in two dimensional photonic quasi-crystals," *Phys. Rev. Lett.*, vol. 80, no. 5, pp. 956–959, Feb. 1998.

[9] C. Jin, B. Cheng, B. Man, Z. Li, and D. Zhang, "Two-dimensional dodecagonal and decagonal quasi-periodic photonic crystals in the microwave region," *Phys. Rev. B*, vol. 61, no. 16, pp. 10 762–10 767, Apr. 2000.

[10] M. E. Zoorob, M. D. B. Charleton, G. J. Parker, J. J. Baumeberg, and M. C. Netti, "Complete photonic bandgaps in 12-fold symmetric quasicrystals," *Nature*, vol. 404, no. 6779, pp. 740–743, Apr. 2000.

[11] M. A. Kaliteevski, S. Brand, R. A. Abram, T. F. Krauss, R. M. De La Rue, and P. Millar, "Two-dimensional penrose-tiled photonic quasicrystals: Diffraction of light and fractal density of modes," *J. Mod. Opt.*, vol. 47, no. 11, pp. 1771–1778, Sep. 2000.

[12] X. Zhang, Z.-Q. Zhang, and C. T. Chan, "Absolute photonic band gaps in 12-fold symmetric photonic quasi-crystals," *Phys. Rev. B*, vol. 63, no. 8, Feb. 2001, 081105(R),.

[13] M. Bayndir, E. Cubukcu, I. Bulu, and E. Ozbay, "Photonic band-gap effect, localization, and waveguiding in the two-dimensional Penrose lattice," *Phys. Rev. B*, vol. 63, no. 16, Apr. 2001, 161104(R),.

[14] M. Hase, H. Miyazaki, M. Egashira, N. Shinya, K. M. Kojima, and S. Uchida, "Isotropic photonic band gap and anisotropic structures in transmission spectra of two-dimensional fivefold and eightfold symmetric quasi-periodic photonic crystals," *Phys. Rev. B*, vol. 66, no. 21, Dec. 2002, 214205,.

[15] Z. Feng, X. Zhang, Y. Wang, Z.-Y. Li, B. Cheng, and D.-Z. Zhang, "Negative refraction and imaging using 12-fold-symmetry quasi-crystals," *Phys. Rev. Lett.*, vol. 94, no. 24, June 2005, 247402,.

[16] F. Przybilla, C. Genet, and T. W. Ebbesen, "Enhanced transmission through Penrose subwavelength hole arrays," *Appl. Phys. Lett.*, vol. 89, no. 12, Sep. 2006, 121115,.

[17] A. Della Villa, V. Galdi, F. Capolino, V. Pierro, S. Enoch, and G. Tayeb, "A comparative study of representative categories of EBG dielectric quasi-crystals," *IEEE Antennas Wireless Propag. Lett.*, vol. 5, pp. 331–334, 2006.

[18] H. Q. Li, Z. H. Hang, Y. Q. Qin, Z. Y. Wei, L. Zhou, Y. W. Zhang, H. Chen H, and C. T. Chan, "Quasi-periodic planar metamaterial substrates," *Appl. Phys. Lett.*, vol. 86, no. 12, Mar. 2005, 121108,.

[19] M. Oxborrow and C. L. Henley, "Random square-triangle tilings: A model for twelvefold-symmetric quasi-crystals," *Phys. Rev. B*, vol. 48, no. 10, pp. 6966–6998, Sep. 1993.

[20] High Frequency Structure Simulator—User's Guide. Pittsburgh, PA, Ansoft Corp., 2003.

[21] S. David, A. Chelnikov, and J.-M. Lourtioz, "Isotropic photonic structures: Archimedean-like tilings and quasi-crystals," *IEEE J. Quantum Electron.*, vol. 37, no. 1, pp. 1427–1434, Nov. 2001.